

EPLIN β Is Involved in the Assembly of Cadherin-catenin Complexes in Osteoblasts and Affects Bone Formation

Shihoko Miyazaki¹, Taro Funamoto¹, Tomohisa Sekimoto¹, Syuji Kurogi¹, Tomomi Ohta¹, Takuya Nagai¹, Takuya Tajima¹, Mai Imasaka², Kumiko Yoshinobu³, Kimi Araki³, Masatake Araki³, Narantsog Choijookhuu⁴, Yoshitaka Hishikawa⁴ and Etsuo Chosa¹

¹Division of Orthopaedic Surgery, Department of Medicine of Sensory and Motor Organs, Faculty of Medicine, University of Miyazaki, Japan, ²Department of Genetics, Hyogo College of Medicine, Japan, ³Institute of Resource Development and Analysis, Kumamoto University, Japan and ⁴Department of Anatomy, Histochemistry and Cell Biology, Faculty of Medicine, University of Miyazaki, Japan

Received March 10, 2022; accepted May 29, 2022; published online June 25, 2022

Epithelial protein lost in neoplasm (EPLIN) is an actin-associated cytoskeletal protein that plays an important role in epithelial cell adhesion. EPLIN has two isoforms: EPLIN α and EPLIN β . In this study, we investigated the role of EPLIN β in osteoblasts using EPLIN β -deficient (*EPLIN β ^{GT/GT}*) mice. The skeletal phenotype of *EPLIN β ^{GT/GT}* mice is indistinguishable from the wildtype (WT), but bone properties and strength were significantly decreased compared with WT littermates. Histomorphological analysis revealed altered organization of bone spicules and osteoblast cell arrangement, and decreased alkaline phosphatase activity in *EPLIN β ^{GT/GT}* mouse bones. Transmission electron microscopy revealed wider intercellular spaces between osteoblasts in *EPLIN β ^{GT/GT}* mice, suggesting aberrant cell adhesion. In *EPLIN β ^{GT/GT}* osteoblasts, α - and β -catenins and F-actin were observed at the cell membrane, but OB-cadherin was localized at the perinuclear region, indicating that cadherin-catenin complexes were not formed. EPLIN β knockdown in MC3T3-e1 osteoblast cells showed similar results as in calvaria cell cultures. Bone formation markers, such as *RUNX2*, *Osterix*, *ALP*, and *Col1a1* mRNA were reduced in EPLIN β knockdown cells, suggesting an important role for EPLIN β in osteoblast formation. In conclusion, we propose that EPLIN β is involved in the assembly of cadherin-catenin complexes in osteoblasts and affects bone formation.

Key words: LIMA1, EPLIN β , OB-cadherin, cell adhesion, osteoblast

I. Introduction

Intercellular interaction and communication are important in multicellular organisms to ensure functional development and differentiation [14, 17]. Osteoblasts are mononuclear, non-terminally differentiated and specialized cells that are arranged in a single layer adherent to

periosteal or endosteal bone surfaces. The alignment and interaction of osteoblasts are important events for bone formation and mineralization. It has been reported that gap junctions, tight junctions, and adherens junctions are involved in intercellular communication of osteoblast lineages [2, 4, 37]. Adherens junctions are intercellular structures that allow homophilic, calcium-dependent cell-cell adhesion via cadherins, which are transmembrane proteins containing Ca²⁺-dependent homophilic adhesion receptors that play important roles in cell recognition and cell fate during development [21, 40]. It has been reported that some cadherin family members, such as OB-cadherin

Correspondence to: Etsuo Chosa MD., Ph.D., Division of Orthopaedic Surgery, Department of Medicine of Sensory and Motor Organs, Faculty of Medicine, University of Miyazaki, 5200 Kihara, Kiyotake, Miyazaki 889–1692, Japan. E-mail: chosa@med.miyazaki-u.ac.jp

(known as cadherin-11), play an important role in the regulation of osteoblast differentiation and osteoid matrix mineralization in osteoblasts [12, 34, 36].

We developed an efficient screening system for identifying novel genes involved in bone metabolism using mutant mouse strains established by an exchangeable gene trap method based on the Exchangeable Gene Trap Clones (EGTC) database [26]. As a result of the screening, we selected epithelial protein lost in neoplasm (EPLIN) as a target molecule. EPLIN, which is a product of the LIMA1 gene, is a cytoskeletal protein that was initially identified as the product of a gene transcriptionally downregulated in oral cancer cell lines [5]. EPLIN is known to bind to actin fibers via α -catenin and link the cadherin-catenin complex to F-actin, thus actively stabilizing the actin bundles and playing important roles in cell adhesion and the formation of adherence junctions to bind cells [13, 29]. These functions of EPLIN have been demonstrated in epithelial, endothelial, and cancer cells [7, 38]. However, the role of EPLIN in osteoblast function has not yet been clarified.

EPLIN exists in two isoforms: EPLIN α , which consists of 600 amino acids, and EPLIN β , which has 759 amino acids [6, 30]. The EPLIN gene consists of 11 exons and has distinct promoters for the two isoforms. EPLIN β mRNA consists of all 11 exons, while EPLIN α mRNA consists of exons 4–11, and the expression of the two isoforms is regulated independently. EPLIN α is a cytoskeletal protein whose expression is often lost in cancerous cells, including metastatic cells [23, 30]. Recently, EPLIN β has been reported to play an important role as a controller of stress fiber formation and stability in endothelial cells [38]. However, the isoform-specific role of EPLIN β in bone structure and function has remained unclear.

In the present study, we first investigated the role of EPLIN β in bone formation and cell adhesion using WT and EPLIN $\beta^{GT/GT}$ mice. Bone morphological changes were demonstrated by hematoxylin and eosin (HE) staining, alkaline phosphatase (ALP) staining, and transmission electron microscopy, whereas the functional activity of osteoblast cells was evaluated by ALP assay and staining. The role of EPLIN β in cell adhesion was examined by immunofluorescence in osteoblast cells. Finally, the *in vivo* experimental findings were confirmed by EPLIN β knock-down experiments *in vitro*.

II. Materials and Methods

Animals and tissue preparation

All experiments using mice were performed with the approval of the Animal Care and Use Committee and the Genetic Modification Safety Committee of Kumamoto University and the University of Miyazaki in accordance with the institutional Guidelines for Animal Experiments and Safety Management Rules for Genetic Modification. We generated EPLIN $\beta^{GT/GT}$ mice to investigate the role of EPLIN β in bone metabolism. For HE and ALP stainings,

11-day-old WT and EPLIN $\beta^{GT/GT}$ mouse femoral bones were used.

Western blot analysis

Cell lysates containing 20 μ g of protein were mixed with loading solution [250 mM Tris/HCl (pH 6.8), 0.5 M sucrose, 5 mM EDTA, 0.006% bromophenol blue, 2-mercaptoethanol, and 4% SDS], boiled for 5 min, and separated by SDS-PAGE with an 8% gradient gel according to previous reports [8, 28]. Samples were electrophoretically transferred onto iBlot (iBlot[®] Gel Transfer Device, Thermo Fisher Scientific Waltham, MA, USA) for dry protein transfer and then washed with double-distilled water. The membranes were blocked with 10% Block Ace (UKB80[®], Yukijirushi, Hokkaido, Japan) at room temperature for 1 hr. Membranes were then incubated overnight at 4°C with rabbit polyclonal EPLIN antibody (EPLIN antibody NB100-2305, Novus Biologicals, Cambridge, UK) and beta-actin (β -actin, polyclonal antibody 20536-1-AP, Proteintech, Chicago, IL, USA), diluted 1:2,500 and 1:1,600 with Can Get Signal[®] Immunoreaction Enhancer Solution 1 (NKB-101, Toyobo, Osaka Japan), respectively. Membranes were then reacted with HRP-goat anti-rabbit IgG antibody (DK-2600, Dako, Glostrup, Denmark) diluted 1:1,000 with Can Get Signal[®] Immunoreaction Enhancer Solution 2 (NKB-201, Toyobo) for 1 hr, prior to being washed three times for 5 min each with PBST/0.05% Triton X-100 buffer. The bands were then visualized with 3,3'-diaminobenzidine (DAB), 1 M PB, 1% NiSO₄, 1% CoCl₂, and 30% H₂O₂ [8].

Micro-computed tomography

To analyze the bone structure, soft tissues surrounding the femur were removed prior to micro-computed tomography (μ CT) scanning, which was performed using a μ CT system (ScanXmate-L090H; Comscantecno, Kanagawa, Japan) as described previously [11, 15, 26]. Bone morphometric analysis was performed on the trabecular bone of the distal femur at 16 weeks after birth (n = 5). The measurement area was set 0.2 mm from the growth plate to 2 mm into the proximal area. For the cortical bone analysis, the mid-point of the femur was scanned. Data from the μ CT scans were analyzed and calculated using a three-dimensional image analyzing system (TRI/3D-BON; Ratoc System Engineering Co. Ltd., Tokyo, Japan). Bone morphometry analysis included trabecular bone mineral content (T.BMC), trabecular bone mineral density Tb.BMD, trabecular bone volume/total volume (BV/TV), trabecular bone thickness (Tb.Th), trabecular bone number (Tb.N), and trabecular separation (Tb.SP). For the cortical bone analysis, cortical bone volume (Ct.V) and cortical bone thickness (Ct.Th) were included.

Biomechanical strength analysis

To determine bone strength, a three-point bending test (EZ-test S; Shimadzu Co., Kyoto, Japan) was conducted on

the excised femur as described previously [15, 26]. The span of the two support points was 6 mm. The deformation rate was 1.0-mm/min. Maximal load (N), displacement (mm), and work to failure (mJ) were obtained from the load-deformation curves.

Transmission electron microscopy

The femur tissue was dissected from 9-day-old WT and *EPLIN β ^{GT/GT}* mice and fixed in 2.5% glutaraldehyde in 0.1 M cacodylate buffer and 2% osmium tetroxide in 0.1 M cacodylate buffer. Bone specimens were dehydrated in a graded ethanol series and embedded in epoxy resin. The specimens were cut into 90- to 95-nm-thick sections, stained with uranyl acetate and lead citrate, and observed using a transmission electron microscope (TEM) Hitachi 7100 (Hitachi, Tokyo, Japan) [15].

Immunofluorescence staining

Cells cultured on glass coverslips were rinsed several times in Ca²⁺- and Mg²⁺-containing PBS, fixed in 4% paraformaldehyde (PFA) for 10 min at 37°C, and permeabilized in 4% PFA containing 0.1% Triton X-100 for 1 min at room temperature. After blocking in 4% Block Ace solution (Yukijirushi Inc., Sapporo, Japan), the cells were incubated for 1 hr separately with primary antibodies: OB-cadherin (#4442; Cell Signaling Technology, Beverly, MA, USA) at 1:100 dilution; and EPLIN (16639-1-AP; Proteintech, Rosemont, IL, USA), β -catenin (H102 sc-7199; Santa Cruz, Dallas, TX, USA) and α -catenin (anti- α 1 catenin antibody EP1793Y; Abcam, Cambridge, UK) all at a dilution of 1:50. After washing, bound antibodies were detected using Alexa Fluor 488-labeled anti-rabbit secondary antibody (Thermo Fisher Scientific) for 30 min. Then, F-actin (Phalloidin, Thermo Scientific) was stained in all slides. Cell nuclei were stained with DAPI (SlowFade Gold Antifade Mountant with DAPI; Thermo Fisher Scientific). As a negative control, normal rabbit IgG was used at the same concentration instead of the primary antibody in each experiment. Microphotos were taken using a fluorescence microscope (BZ-9000; Keyence, Osaka, Japan).

Calvaria cell cultures

Osteoblast-enriched calvaria cultures were prepared from 3- to 4-day-old WT and *EPLIN β ^{GT/GT}* mice by sequential collagenase digestion as previously described [31, 33]. The calvaria was digested with 0.1% collagenase (Wako Pure Chemical Industries, Osaka, Japan) and 0.2% dispase (Gibco, Thermo Fisher Scientific) at 37°C for 10 min. The solution was moved to a fresh sterile tube (fraction 1). This procedure was repeated five more times with fresh solution (fractions 2–4). Fractions 2–4 were then combined, and the cells were pelleted by centrifugation at 15,000 \times g for 5 min. The isolated cells were grown in alpha-modified Eagle's medium (α -MEM; Gibco BRL) supplemented with 10% fetal bovine serum (FBS). The medium was changed every three days, and the cell culture

supernatant was collected 24 hr after the last medium change. A total of 8×10^5 cells/ml were plated and maintained in α -MEM supplemented with 10% FBS, 100 ng/ml bone morphogenetic protein (BMP)-2 (Sigma-Aldrich, St. Louis, MO, USA), 50 μ g/ml ascorbic acid, and 5 mM β -glycerophosphate for six weeks. Cells were then maintained in α -MEM with 10% FBS, and the medium was changed twice a week.

Quantitative real-time polymerase chain reaction

Total RNA was extracted from the MC3T3-e1 osteoblastic cell line using the ReliaPrep RNA Tissue Miniprep System (Promega) and reverse transcribed into cDNA using M-MLV Reverse Transcriptase (Invitrogen, Carlsbad, CA, USA). Gene expression levels were analyzed by the $\Delta\Delta$ CT method using the SYBR Green and Step One Plus PCR system (Thermo Fisher Scientific). All samples were assayed in triplicate, and the CT values were averaged. GAPDH was used as the internal control. The CT values of the target genes were compared with control siRNA-transfected cells at day one. Primer sequences EPLIN α F-5'-GCAGTAACTGTTACAGCTGTGTG-3' and R-5'-CAGCCAAACATGCGTCTTTG-3', EPLIN β F-5'-TCTAGTCAGCCCACAGGTGTCTC-3' and R-5'-TCAATGACAGGGAAGTCCACTG-3', RUNX2 F-5'-TACAAACCATACCCAGTCCCCTGTTT-3' and R-5'-AGTGCTCTAACCACAGTCCATGCA-3', Osterix F-5'-ATGGCGTCTCTCTGCTTG-3' and R-5'-TGAAAGGTCAGCGTATGCTT-3', ALP F-5'-CCAACTCTTTTGTGCCAGAGA-3' and R-5'-GGCTACATTGGTGTGAGCTTTT-3', OB Cadherin F-5'-TGAAGATAGAGGCCGCAAT-3' and R-5'-CCAAGAACATGGGAGGCTCAT-3', and Col1a1 F-5'-GCTCCTCTTAGGGGCCAC T-3' and R-5'-CCACGTCTCACCATTGGGG-3' β -actin F-5'-GAGCTATGAGCTGCCTGACG-3' and R-5'-AGTTTCATGGATGCCACAGG-3'.

EPLIN β knockdown experiment

The murine osteoblastic cell line MC3T3-e1 was purchased from RIKEN (RIKEN BioResource Center, Wako, Japan). For transfection, MC3T3-e1 cells were divided into two groups, including control-siRNA and EPLIN β -siRNA. Transfection was performed using Lipofectamine RNA iMAX (Invitrogen), and all transfection operations were performed in strict accordance with Lipofectamine RNA iMAX transfection instructions. Cells that were successfully transfected were prepared into cell suspensions using α -MEM with L-Glutamine and Phenol Red with 10% FBS and 100 ng/ml, 50 μ g/ml ascorbic acid, and 5 mM β -glycerophosphate. They were seeded at a density of 2×10^4 cells per well in 24-well plates, followed by incubation in a constant temperature incubator (5% CO₂, 37°C, 95% humidity). Then, the expression of EPLIN β was detected by quantitative real-time polymerase chain reaction (qRT-PCR) after transfection for three days.

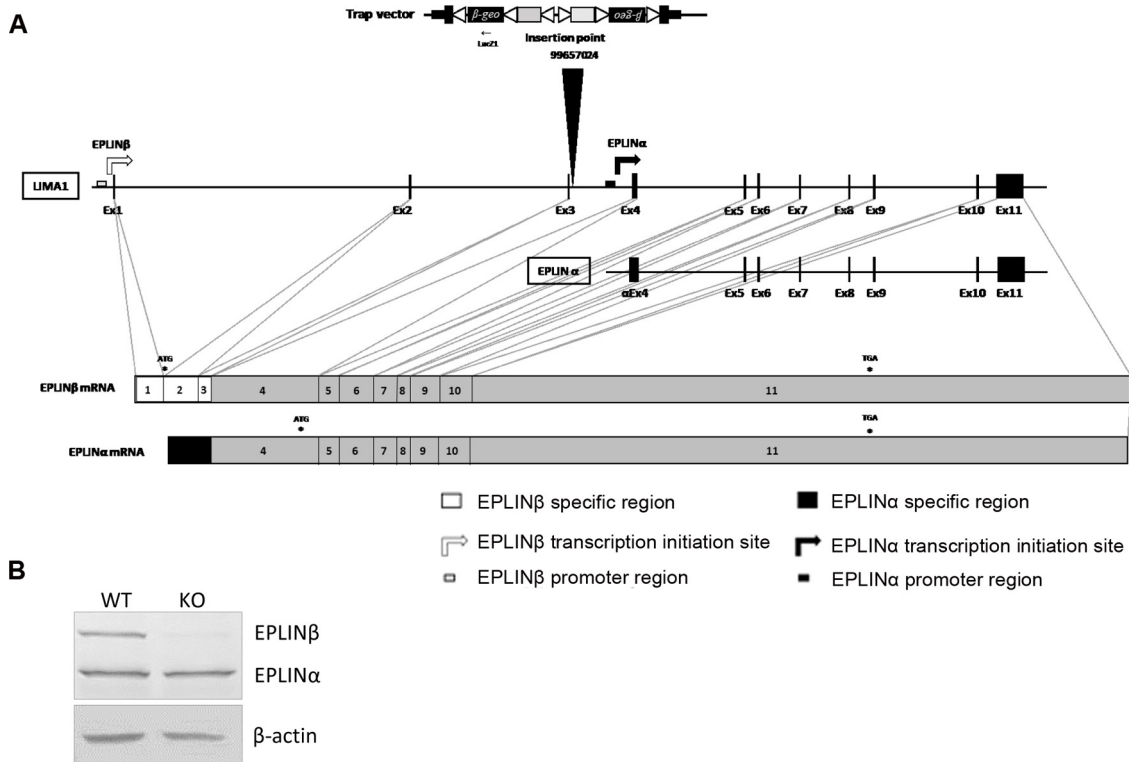


Fig. 1. Generation of *EPLINβ^{GT/GT}* mice. **(A)** Map of the *EPLINβ^{GT/GT}* allele. *EPLINα* and *EPLINβ* mRNA are transcribed from distinct promoters, not alternative splicing. The insertion point was upstream of the *EPLINα* promoter region in intron 3. **(B)** Western blot analysis of EPLIN in WT and *EPLINβ^{GT/GT}* mouse lung tissues. *EPLINα* (76.4 kDa), *EPLINβ* (90.8 kDa), and β -actin (42 kDa) bands were detected.

ALP assay and staining

Alkaline phosphatase (ALP) activity was examined in the MC3T3-e1 osteoblastic cell line after three days of transfection with control-siRNA and *EPLINβ*-siRNA using a TRACP&ALP Assay Kit (Takara Bio, Japan). In bone tissue sections and cultured cells, ALP expression was examined using a TRAP/ALP staining kit (Fujifilm Wako Chemicals, Osaka, Japan) according to the manufacturer's protocol.

Statistical analyses

The data were analyzed by Student's *t*-test using Statistical Package for Social Sciences (version 20; IBM Corp., Armonk, NY, USA). The data in the graphs are presented as the mean \pm standard deviation. *P* values of <0.05 were considered to indicate statistical significance.

III. Results

Generation and validation of *EPLINβ^{GT/GT}* mice

EPLINβ mRNA requires all 11 exons, while *EPLINα* mRNA requires exons 4–11. *EPLINα* and *EPLINβ* mRNA are transcribed from distinct promoters, not alternative splicing, and the promoter region of *EPLINα* is near upstream exon 4 [6, 10]. Two pU-21W gene trap vectors were inserted 6.5 kb upstream of exon 4 (Fig. 1A). From

the position of the insertion point and the promoter region, there was possible deficiency of *EPLINα*, *EPLINβ*, or both. Western blot (WB) was performed to investigate the EPLIN expression, which is a product of the *LIMA1* gene. As a result, both *EPLINα* and *EPLINβ* were expressed in WT mouse (Fig. 1B). However, only *EPLINα* was detected in knockout mouse bone. This result confirms that *EPLINβ* was deficient in *EPLINβ^{GT/GT}* mice.

Bone morphometric analysis in *EPLINβ^{GT/GT}* mice

Micro-CT scans of the femurs were performed on 16-week-old WT and *EPLINβ^{GT/GT}* mice. Bone masses in trabecular bones of the distal femur were significantly decreased in the *EPLINβ^{GT/GT}* mice compared with WT mice (Fig. 2A). In biomechanical strength analysis, the maximum load was significantly decreased in *EPLINβ^{GT/GT}* mice compared with WT mice, confirming significant bone fragility in *EPLINβ^{GT/GT}* mice (Fig. 2B). Trabecular bone parameters including trabecular bone mineral content (T.BMC), trabecular bone mineral density (Tb.BMD), trabecular bone thickness (Tb.Th), and trabecular bone number (Tb.N) were significantly decreased in *EPLINβ^{GT/GT}* mice compared with WT littermates (Fig. 2C). Trabecular separation (Tb.Sp), which is the parameter of the cavities containing the trabecular region, showed an increasing trend in *EPLINβ^{GT/GT}* mice. Moreover, cortical bone thick-

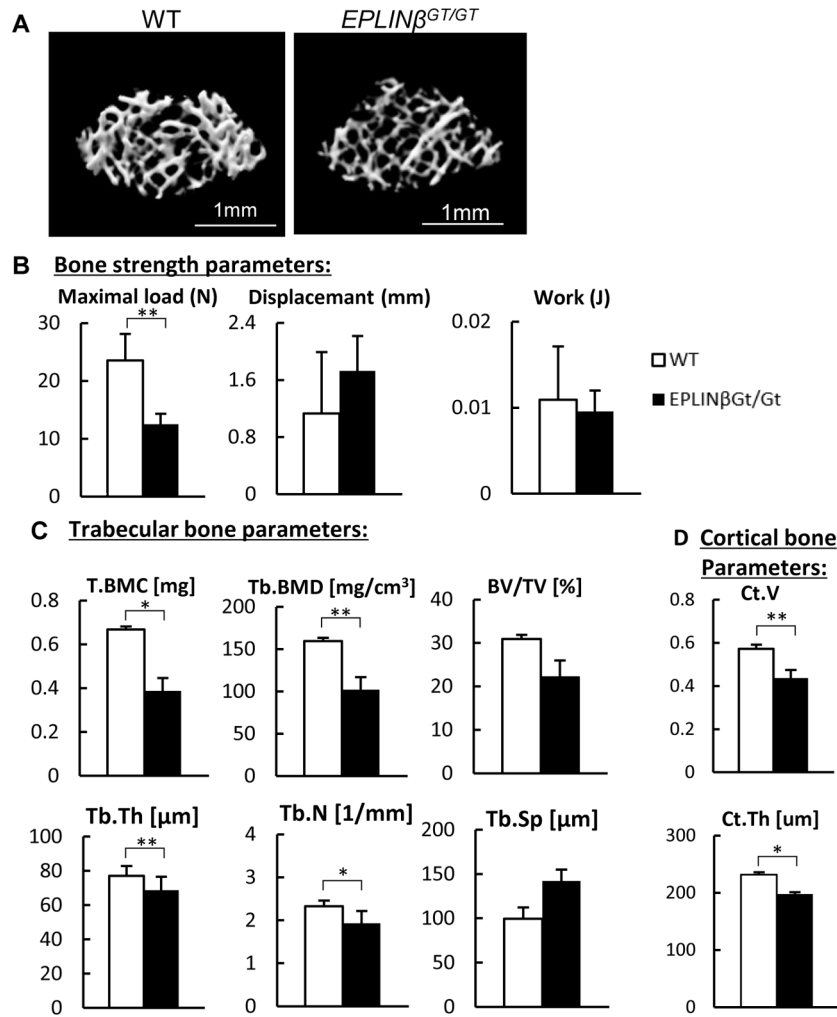


Fig. 2. Bone morphometric analysis. (A) Micro-CT scans of WT and *EPLIN* $\beta^{GT/GT}$ mouse femur bones. Bar = 1 mm. (B) Bone strength parameters were revealed, including maximal load, maximum displacement, and maximum work. Trabecular bone parameters (C), trabecular bone mineral content (T.BMC), trabecular bone mineral density Tb.BMD, trabecular bone volume/total volume (BV/TV), trabecular bone thickness (Tb.Th), trabecular bone number (Tb.N), trabecular separation (Tb.SP), cortical bone parameters (D), cortical bone volume (Ct.V), and cortical bone thickness (Ct.Th) were compared in WT and *EPLIN* $\beta^{GT/GT}$ mouse bones. Data represent the mean \pm SD of three independent experiments. * $P < 0.05$, ** $P < 0.01$.

ness (Ct.Th) and cortical bone volume (Ct.V) were significantly decreased in *EPLIN* $\beta^{GT/GT}$ mice (Fig. 2D).

Histomorphological analysis of *EPLIN* $\beta^{GT/GT}$ mouse bones

For detailed analysis of bone morphology, WT and *EPLIN* $\beta^{GT/GT}$ mouse femur bones were examined by HE staining. In *EPLIN* $\beta^{GT/GT}$ mouse bones, reduced staining intensity of the bone matrix and altered organization of bone spicules and osteoblast cell arrangement were observed compared to WT littermates (Fig. 3A). Functional activity of osteoblast cells was examined by ALP staining (Fig. 3B). In the WT mice, trabecular and cortical bone regions were intensely stained. However, in *EPLIN* $\beta^{GT/GT}$ mice, only weak ALP staining was observed in the same regions. Next, the ultrastructure of mouse trabecular bones was examined by TEM (Fig. 3C). In WT mice, osteoblast morphology and intercellular spaces were uniform. The

nuclei of osteoblast cells were localized just below the intercellular adhesion site, and intracellular organelles, such as the rough endoplasmic reticulum (rER), Golgi apparatus, and mitochondria were abundantly observed in each cell. In *EPLIN* $\beta^{GT/GT}$ mice, osteoblast cells were localized sparsely due to altered intercellular junctions (Fig. 3C, asterisks). Moreover, osteoblast cytoplasm became thin, whereas intercellular spaces became wider, and pseudopodia-like structures were observed at the cell membranes.

Subcellular localization of junctional proteins in osteoblasts

The subcellular localization of EPLIN was examined by immunofluorescence in osteoblast cultures derived from WT and *EPLIN* $\beta^{GT/GT}$ mouse calvaria. In WT osteoblasts, EPLIN was mostly co-localized with F-actin around the cell membrane (Fig. 4A). However, in *EPLIN* β -depleted cells, significantly decreased expression was found, which

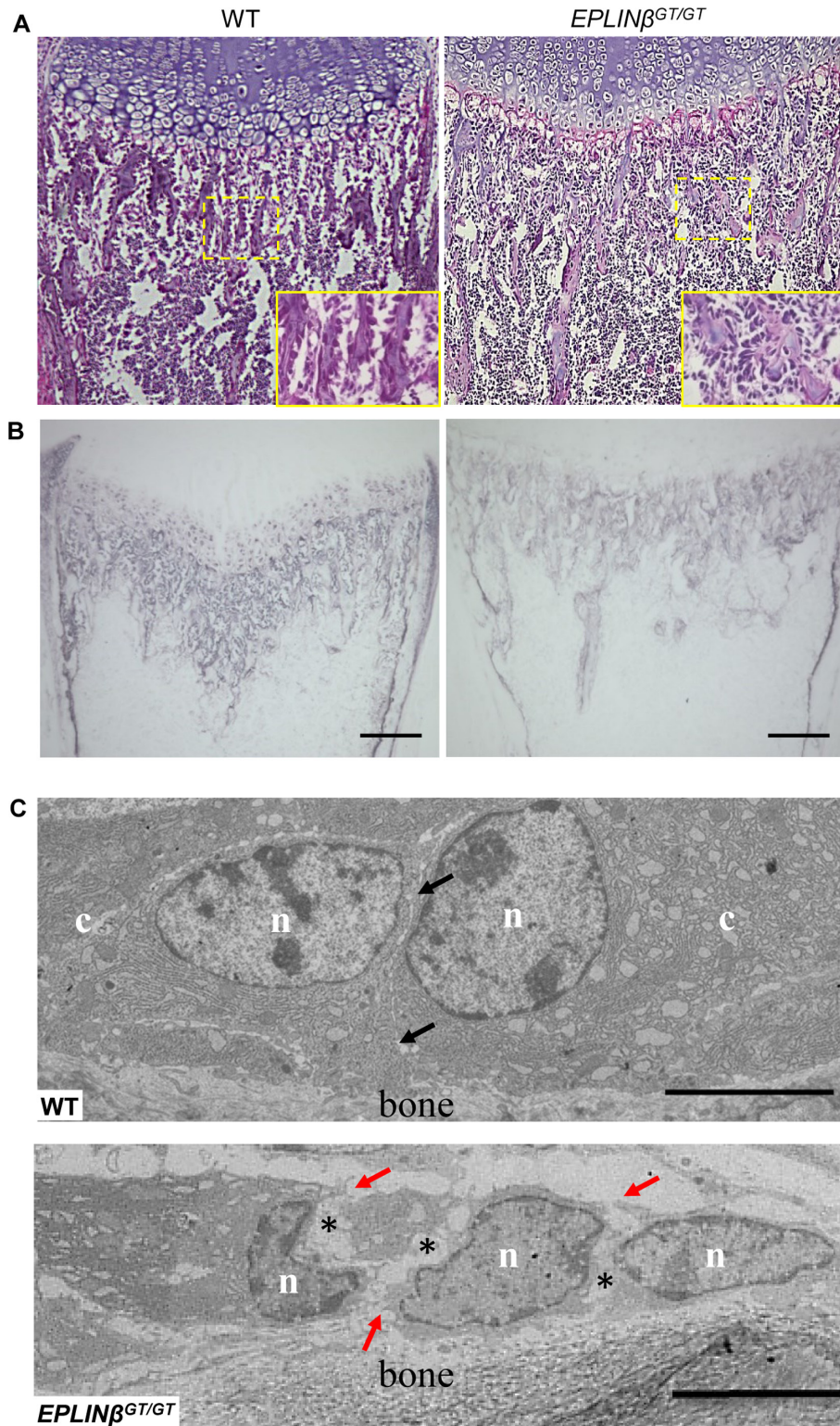


Fig. 3. Histomorphological analysis of *EPLIN* $\beta^{GT/GT}$ mouse bones. (A) HE staining of 11-day-old WT and *EPLIN* $\beta^{GT/GT}$ mouse femoral bones. Dashed line areas are enlarged in the inset. (B) ALP staining of WT and *EPLIN* $\beta^{GT/GT}$ mouse femoral bones. Scale bar, 200 μ m. (C) TEM of 9-day-old WT and *EPLIN* $\beta^{GT/GT}$ mouse femoral bones. Osteoblast cell nuclei (n), cytoplasm (c), and cellular junctions (black arrow) are marked. Asterisks indicate aberrant cellular junctions between osteoblasts. Pseudopodia-like structures are present between intercellular spaces (red arrow). Bar = 5 μ m.

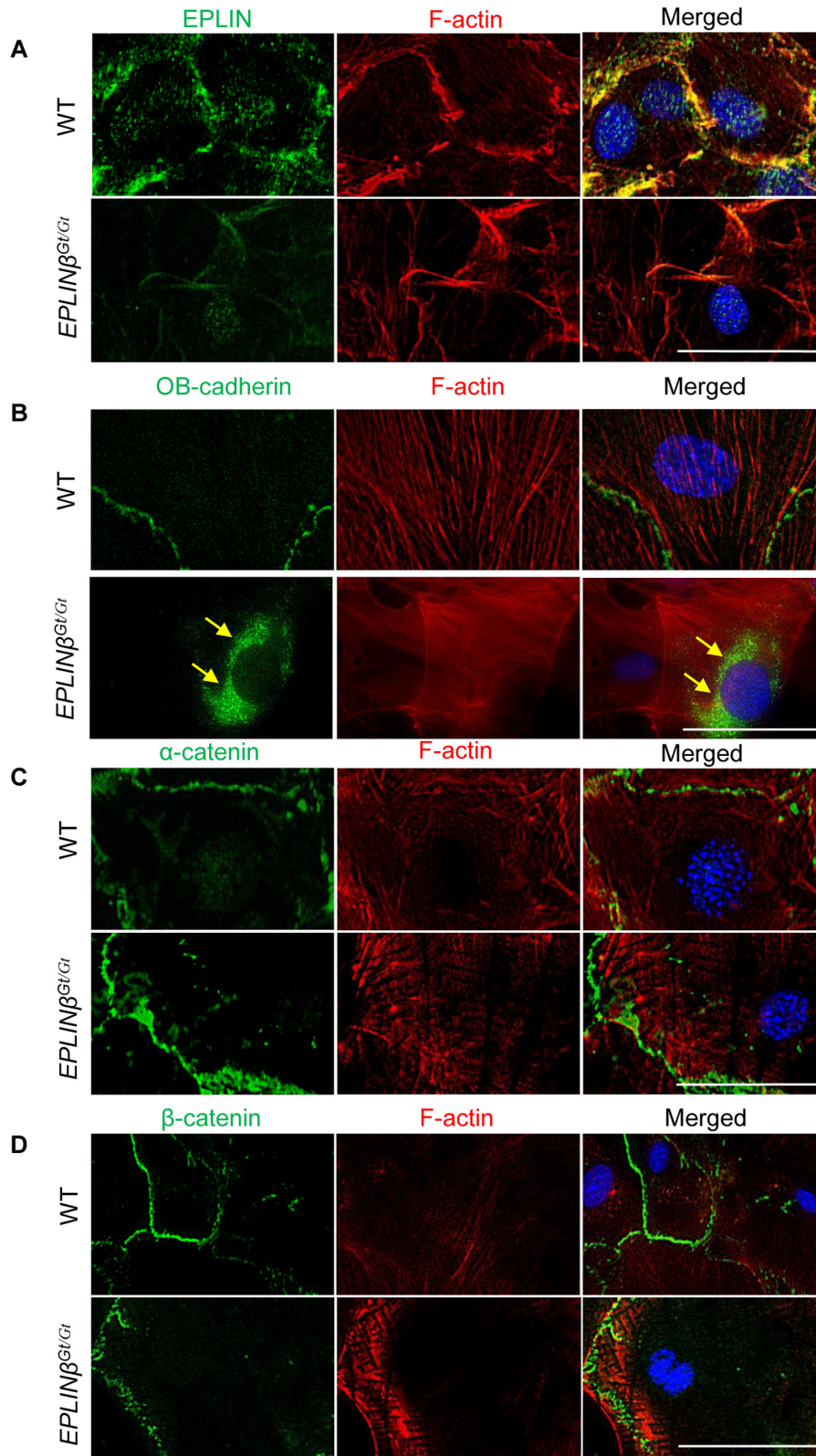


Fig. 4. Expression of junctional proteins in osteoblast-enriched calvaria cultures. Osteoblast cells were prepared from WT and *EPLIN* $\beta^{GT/GT}$ mice. The expressions of EPLIN (A), OB-cadherin (B), α -catenin (C), and β -catenin (D) were examined by immunofluorescence. Arrows indicate the perinuclear localization of OB-cadherin. In each specimen, cellular cytoskeletons were stained by F-actin (red staining). Cell nuclei were counterstained by DAPI. Microphotos represent three independent experimental results. Bar = 50 μ m.

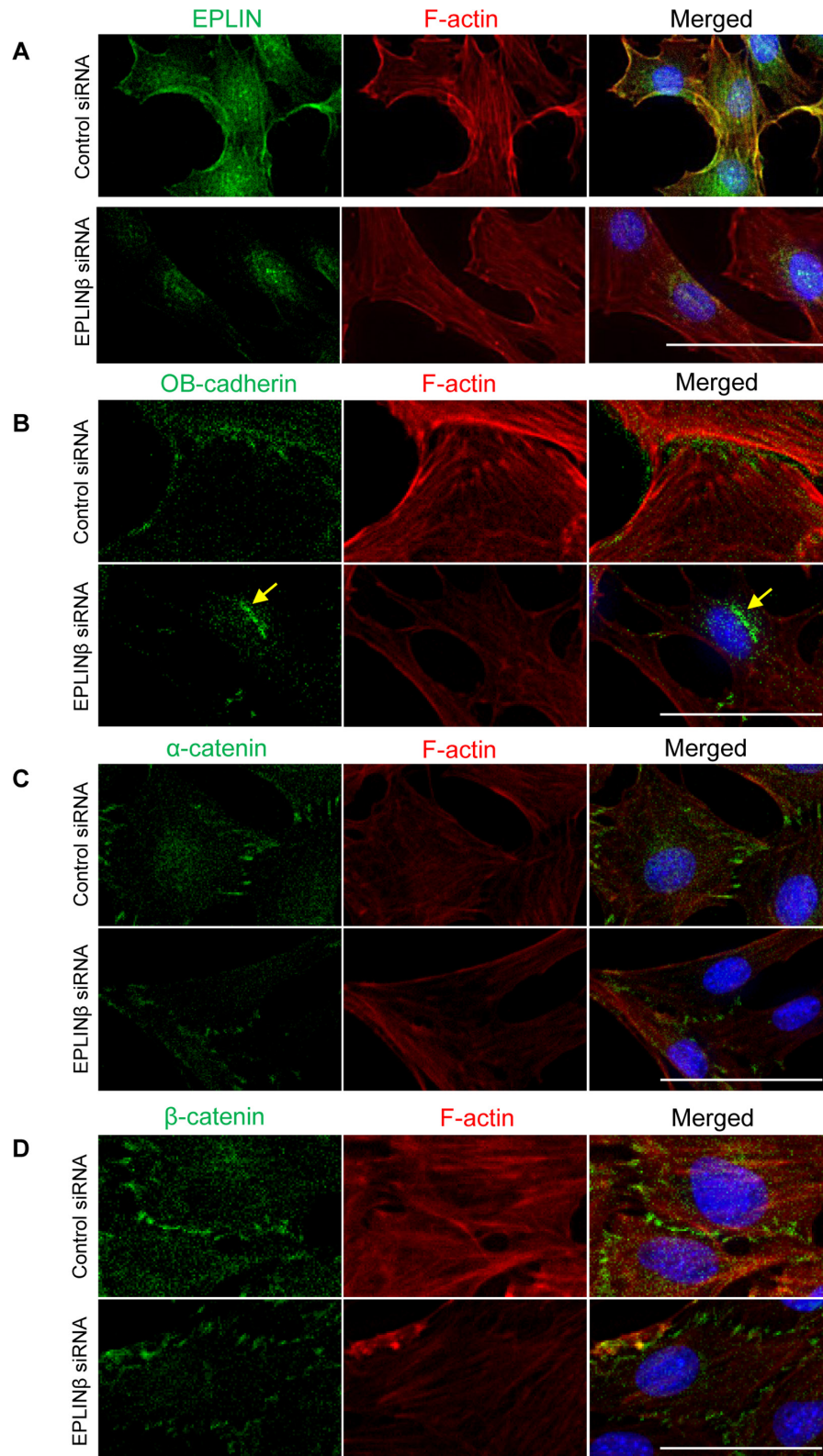


Fig. 5. Expression of junctional proteins in the MC3T3-e1 osteoblastic cell line. Control-siRNA and EPLIN β -siRNA were transfected into MC3T3-e1 osteoblastic cells. The expressions of EPLIN (A), OB-cadherin (B), α -catenin (C), and β -catenin (D) were examined by immunofluorescence. Arrows indicate the perinuclear localization of OB-cadherin. In each specimen, cellular cytoskeletons were stained by F-actin (red staining). Cell nuclei were counterstained by DAPI. Microphotos represent three independent experimental results. Bar = 50 μ m.

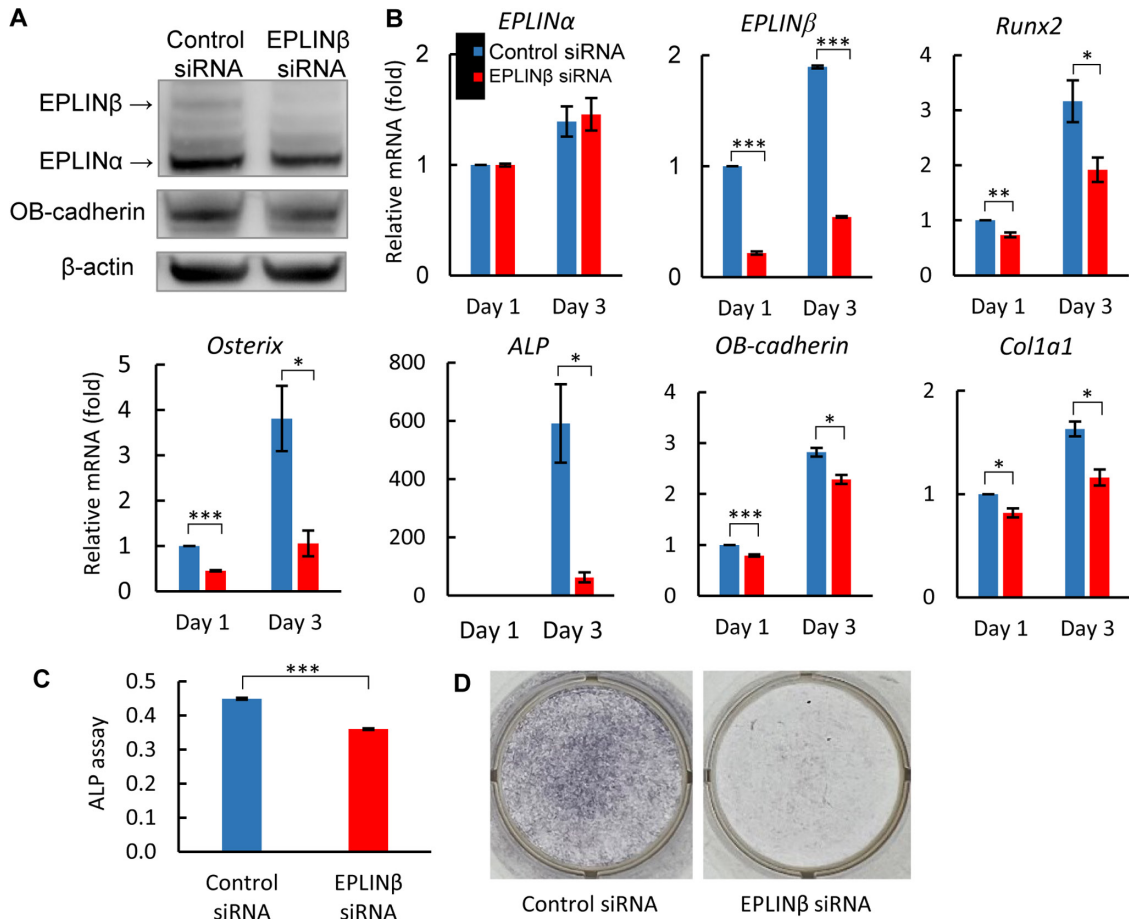


Fig. 6. EPLIN β knockdown in osteoblast cells. (A) WB analysis of MC3T3-e1 osteoblast cells transfected with control and EPLIN β siRNA. EPLIN α (76.4 kDa), EPLIN β (90.8 kDa), OB-cadherin (110 kDa), and β -actin (42 kDa) bands were detected. (B) qRT-PCR of *EPLIN α* , *EPLIN β* , *RUNX2*, *Osterix*, *ALP*, and *Col1a1* mRNA in osteoblast cell cultures transfected with control and EPLIN β siRNA. (C) ALP assay in MC3T3-e1 osteoblastic cells three days after transfection with control and EPLIN β siRNA. (D) ALP staining of MC3T3-e1 osteoblastic cells three days after transfection with control and EPLIN β siRNA. Data represent the mean \pm SD of three independent experiments. * $P < 0.05$, ** $P < 0.01$, *** $P < 0.001$.

indicates the remaining EPLIN α expression in osteoblasts. Next, we examined the localization of junctional proteins. In WT osteoblasts, OB-cadherin was localized at the cell membrane (Fig. 4B). Surprisingly, OB-cadherin had its localization changed to the perinuclear region in EPLIN $\beta^{GT/GT}$ osteoblasts (arrows). There was no change in the expressions of α -catenin and β -catenin in EPLIN $\beta^{GT/GT}$ osteoblasts (Fig. 4C, D).

To confirm these *in vivo* experimental findings, we performed EPLIN β knockdown experiments using the MC3T3-e1 osteoblastic cell line (Fig. 5A). In control siRNA transfected cells, EPLIN expression was mainly co-localized with F-actin in cell membranes. Successful EPLIN β knockdown was confirmed in EPLIN β siRNA-transfected cells. The localization of OB-cadherin was also changed to the perinuclear region in EPLIN β knockdown cells (arrows in Fig. 5B). The expression of α -catenin and β -catenin was not changed in EPLIN β knockdown cells (Fig. 5C, D).

The effects of EPLIN β knockdown in osteoblast cells

Knockdown efficiency was confirmed in control and EPLIN β siRNA-transfected cells using WB analysis (Fig. 6A). In EPLIN β -transfected cells, the successful knockdown of EPLIN β was confirmed, whereas EPLIN α was intact (Fig. 6B). qPCR analysis also confirmed these findings of no changes in *EPLIN α* mRNA expression and significantly decreased expression of *EPLIN β* mRNA in EPLIN β knockdown cells. Next, we examined the expressions of genes important for bone formation and function. In EPLIN β knockdown cells, the expressions of *Runx2*, *Osterix*, *ALP*, *OB-cadherin*, and *Col1a1* mRNAs were significantly decreased at days 1 and 3. In EPLIN β knockdown cells, the ALP activity was significantly decreased comparing to control siRNA-transfected cells (Fig. 6C). Moreover, a significant decrease in ALP staining was confirmed in EPLIN β knockdown cells (Fig. 6D).

IV. Discussion

This is the first study to investigate the role of EPLIN β in mouse bones. The main finding in this study is the important role of EPLIN β in the assembly of cadherin-catenin complexes in osteoblasts. In the absence of EPLIN β , aberrant cadherin-catenin complexes induced abnormal cellular junctions that resulted in altered bone formation.

We designed a unique screening system to detect genes that are important for bone metabolism, and EPLIN β was found as a result [26]. In this study, WB revealed the presence of EPLIN α and absence of EPLIN β , indicating the successful generation of EPLIN $\beta^{GT/GT}$ mice. Morphological abnormalities were found in EPLIN $\beta^{GT/GT}$ mouse bones, while EPLIN α expression was intact. These results suggest that EPLIN α and EPLIN β have distinct functional roles in mouse bones, and EPLIN α does not compensate for the absence of EPLIN β .

EPLIN β -deficient mice were not obviously different from their WT littermates, but the bone mass and strength of the long bones were significantly decreased in comparison. The reason for this difference was examined by histomorphological analysis, and reduced staining intensity of the bone matrix and altered organization of bone spicules and osteoblast cell arrangement were detected. These findings are expected, given that EPLIN is involved in cell adhesion and stabilizes the cytoskeleton by linking to both cadherin-catenin complexes and actin fibers [1, 29]. Ultrastructural analysis revealed aberrant cell adhesion and different sizes of osteoblasts in EPLIN β -deficient mice. Abundant Golgi apparatuses and rER were found in WT osteoblasts, whereas fewer organelles and thin cytoplasm were observed in EPLIN β -deficient osteoblasts, indicating immature differentiation. These results suggest that the differentiation of EPLIN $\beta^{GT/GT}$ osteoblasts is delayed compared to WT osteoblasts.

Adhesion factors such as cadherin and members of the integrin family affect bone formation [12, 18, 25, 36]. In osteoblasts, OB-cadherin, N-cadherin, and P-cadherin are expressed at the cell membrane, with the major molecules being OB- and N-cadherin given their expression level [24]. The phenotypes of mice deficient in each cadherin are different. N-cadherin-null mutant mice are lethal at embryonic day 10 [20, 35], but *OB-cadherin*^{-/-} mice have an indistinct phenotype, with decreased bone volume of the long bone metaphysis [25]. Our results also revealed that OB-cadherin was localized at the perinuclear region, but not in the cell membrane, in EPLIN $\beta^{GT/GT}$ osteoblasts. The skeletal phenotype of EPLIN $\beta^{GT/GT}$ mice is similar to that of *OB-cadherin*^{-/-} mice, but not N-cadherin-null mice. N-cadherin is expressed constitutively, whereas OB-cadherin is expressed selectively in preosteoblasts [24]. Moreover, the expression of OB-cadherin is regulated by semaphorin 4D, which is a signal ligand on osteoclast surfaces [32]. Semaphorin 4D stimulation decreases the expression of

OB-cadherin at the cell membrane in osteoblasts and inhibits bone formation. It has been revealed that intercellular adhesion affects signal transduction to the nucleus [16, 19]. Cadherin is synthesized as pro-cadherin and associate with catenins, then proteolytically processed to create the mature form in the ER or Golgi apparatus [9, 41]. However, cadherin transport has been reported to be non-one-way to the cell membrane. Surface E-cadherins are endocytosed, during which they are either recycled to the cell surface or targeted for degradation [3]. In the present study, cadherin-catenin complexes were not assembled appropriately, and OB-cadherin had perinuclear localization in EPLIN β -deficient osteoblasts. These facts suggest that EPLIN β is involved in bone formation by regulating the distribution of OB-cadherin. Further experiments will be needed to determine how EPLIN is involved in regulating cadherin distribution.

In contrast, the localizations of α - and β -catenins were normal in both WT and EPLIN β -deficient osteoblasts. The gene expressions essential for bone formation and function were significantly decreased in EPLIN β knockdown cells. These results indicate the importance of EPLIN β for bone formation. Decreased ALP activity in both *in vivo* and *in vitro* experiments suggests impaired functional activity in EPLIN β -deficient osteoblasts. However, bone and other organs are closely influenced by each other [39, 27], and since EPLIN $\beta^{GT/GT}$ mice are systemically deficient in this gene, the possibility of secondary effects cannot be ruled out. Further investigation is needed to clarify the role of EPLIN β .

In environments such as gravity and muscle tension, bone has trabeculae formed in response to its stress. Under these conditions, osteoblasts cooperate with osteoclasts to form and maintain their structure. Recently, EPLIN β have reported to be the control of stress fiber formation and stability in endothelial cell in aorta but not vena cava [38]. Therefore, stress-related EPLIN β may be important in osteoblasts [22]. Despite our data showing that EPLIN α was expressed in EPLIN $\beta^{GT/GT}$ mice, EPLIN $\beta^{GT/GT}$ osteoblasts exhibited impaired cell differentiation and intercellular adhesion suggest that EPLIN β is an important isoform in osteoblasts.

In summary, we demonstrated the role of EPLIN β in osteoblast cell adhesion and bone formation. EPLIN β deficiency affected subcellular localization of OB-cadherin, which is an important component of the cadherin-catenin complex.

V. Conflict of Interest

The authors declare that no conflicts of interest exist.

VI. Acknowledgments

We thank W. Souma, I. Tsuchimochi, M. Nagata, M. Yano, for technical support in the laboratory. This work

was supported by the Program for Promotion of Fundamental Studies in Health Sciences of the National Institute of Biomedical Innovation of Japan, a Grant of Japan Orthopaedics and Traumatology Foundation, Inc., nos. 195 and 288, and JSPS KAKENHI Grant Numbers 23592220, 24592271, 26462334, 26462305, 26670669, and 15K10485.

VII. References

- Abe, K. and Takeichi, M. (2008) EPLIN mediates linkage of the cadherin catenin complex to F-actin and stabilizes the circumferential actin belt. *Proc. Natl. Acad. Sci. U S A* 105; 13–19.
- Arana-Chavez, V. E., Soares, A. M. and Katchburian, E. (1995) Junctions between early developing osteoblasts of rat calvaria as revealed by freeze-fracture and ultrathin section electron microscopy. *Arch. Histol. Cytol.* 58; 285–292.
- Bryant, D. M. and Stow, J. L. (2004) The ins and outs of E-cadherin trafficking. *Trends Cell Biol.* 14; 427–434.
- Campbell, H. K., Maier, J. L. and DeMali, K. A. (2017) Interplay between tight junctions and adherens junctions. *Exp. Cell Res.* 358; 39–44.
- Chang, D. D., Park, N. H., Denny, C. T., Nelson, S. F. and Pe, M. (1998) Characterization of transformation related genes in oral cancer cells. *Oncogene* 16; 1921–1930.
- Chen, S., Maul, R. S., Kim, H. R. and Chang, D. D. (2000) Characterization of the human EPLIN (Epithelial Protein Lost in Neoplasm) gene reveals distinct promoters for the two EPLIN isoforms. *Gene* 248; 69–76.
- Chervin-Pétinot, A., Courçon, M., Almagro, S., Nicolas, A., Grichine, A., Grunwald, D., *et al.* (2012) Epithelial protein lost in neoplasm (EPLIN) interacts with α -catenin and actin filaments in endothelial cells and stabilizes vascular capillary network in vitro. *J. Biol. Chem.* 287; 7556–7572.
- Choi-jookhuu, N., Sato, Y., Nishino, T., Endo, D., Hishikawa, Y. and Koji, T. (2012) Estrogen-dependent regulation of sodium/hydrogen exchanger-3 (NHE3) expression via estrogen receptor β in proximal colon of pregnant mice. *Histochem. Cell Biol.* 137; 575–587.
- Curtis, M. W., Johnson, K. R. and Wheelock, M. J. (2008) E-cadherin/catenin complexes are formed cotranslationally in the endoplasmic reticulum/Golgi compartments. *Cell Commun. Adhes.* 15; 365–378.
- Dawid, I. B., Toyama, R. and Taira, M. (1995) LIM domain proteins. *C. R. Acad. Sci. III* 318; 295–306.
- Dempster, D. W., Compston, J. E., Drezner, M. K., Glorieux, F. H., Kanis, J. A., Malluche, H., *et al.* (2013) Standardized nomenclature, symbols, and units for bone histomorphometry: a 2012 update of the report of the ASBMR Histomorphometry Nomenclature Committee. *J. Bone Miner. Res.* 28; 2–17.
- Di Maggio, N., Martella, E., Frismantiene, A., Resink, T. J., Schreiner, S., Lucarelli, E., *et al.* (2017) Extracellular matrix and $\alpha 5\beta 1$ integrin signaling control the maintenance of bone formation capacity by human adipose-derived stromal cells. *Sci. Rep.* 7; 44398.
- Drees, F., Pokutta, S., Yamada, S., Nelson, W. J. and Weis, W. I. (2005) Alpha-catenin is a molecular switch that binds E-cadherin-beta-catenin and regulates actin-filament assembly. *Cell* 123; 903–915.
- Drubin, D. G. and Nelson, W. J. (1996) Origins of cell polarity. *Cell* 84; 335–344.
- Funamoto, T., Sekimoto, T., Murakami, T., Kurogi, S., Imaizumi, K. and Chosa, E. (2011) Roles of the endoplasmic reticulum stress transducer OASIS in fracture healing. *Bone* 49; 724–732.
- Furukawa, K. T., Yamashita, K., Sakurai, N. and Ohno, S. (2017) The Epithelial Circumferential Actin Belt Regulates YAP/TAZ through Nucleocytoplasmic Shuttling of Merlin. *Cell Rep.* 20; 1435–1447.
- Gumbiner, B. M. (1996) Cell adhesion: the molecular basis of tissue architecture and morphogenesis. *Cell* 84; 345–357.
- Hinck, L., Näthke, I. S., Papkoff, J. and Nelson, W. J. (1994) Dynamics of cadherin/catenin complex formation: novel protein interactions and pathways of complex assembly. *J. Cell Biol.* 125; 1327–1340.
- Hirata, H., Samsonov, M. and Sokabe, M. (2017) Actomyosin contractility provokes contact inhibition in E-cadherin-ligated keratinocytes. *Sci. Rep.* 7; 46326.
- Horikawa, K., Radice, G., Takeichi, M. and Chisaka, O. (1999) Adhesive subdivisions intrinsic to the epithelial somites. *Dev. Biol.* 215; 182–189.
- Hynes, R. O. and Lander, A. D. (1992) Contact and adhesive specificities in the associations, migrations, and targeting of cells and axons. *Cell* 68; 303–322.
- Inoue, A., Nakao-Kuroishi, K., Kometani-Gunjigake, K., Mizuhara, M., Shirakawa, T., Ito-Sago, M., *et al.* (2020) VNUT/SLC17A9, a vesicular nucleotide transporter, regulates osteoblast differentiation. *FEBS Open Bio.* 10; 1612–1623.
- Jiang, W. G., Martin, T. A., Lewis-Russell, J. M., Douglas-Jones, A., Ye, L. and Mansel, R. E. (2008) Eplin-alpha expression in human breast cancer, the impact on cellular migration and clinical outcome. *Mol. Cancer* 7; 71.
- Kawaguchi, J., Azuma, Y., Hoshi, K., Kii, I., Takeshita, S., Ohta, T., *et al.* (2001) Targeted disruption of cadherin-11 leads to a reduction in bone density in calvaria and long bone metaphyses. *J. Bone Miner. Res.* 16; 1265–1271.
- Kawaguchi, J., Kii, I., Sugiyama, Y., Takeshita, S. and Kudo, A. (2001) The transition of cadherin expression in osteoblast differentiation from mesenchymal cells: consistent expression of cadherin-11 in osteoblast lineage. *J. Bone Miner. Res.* 16; 260–269.
- Kurogi, S., Sekimoto, T., Funamoto, T., Ota, T., Nakamura, S., Nagai, T., *et al.* (2017) Development of an efficient screening system to identify novel bone metabolism-related genes using the exchangeable gene trap mutagenesis mouse models. *Sci. Rep.* 7; 40692.
- Li, G., Zhang, L., Wang, D., AIQudsy, L., Jiang, J. X., Xu, H., *et al.* (2019) Muscle-bone crosstalk and potential therapies for sarco-osteoporosis. *J. Cell Biochem.* 120; 14262–14273.
- Mai, N., Yamaguchi, Y., Choi-jookhuu, N., Matsumoto, J., Nanashima, A., Takagi, H., *et al.* (2020) Photodynamic Therapy Using a Novel Phosphorus Tetraphenylporphyrin Induces an Anticancer Effect via Bax/Bcl-xL-related Mitochondrial Apoptosis in Biliary Cancer Cells. *Acta Histochem. Cytochem.* 53; 61–72.
- Maul, R. S. and Chang, D. D. (1999) EPLIN, epithelial protein lost in neoplasm. *Oncogene* 18; 7838–7841.
- Maul, R. S., Sachi Gerbin, C. and Chang, D. D. (2001) Characterization of mouse epithelial protein lost in neoplasm (EPLIN) and comparison of mammalian and zebrafish EPLIN. *Gene* 262; 155–160.
- Nakashima, T., Hayashi, M., Fukunaga, T., Kurata, K., Oh-Hora, M., Feng, J. Q., *et al.* (2011) Evidence for osteocyte regulation of bone homeostasis through RANKL expression. *Nat. Med.* 17; 1231–1234.
- Negishi-Koga, T., Shinohara, M., Komatsu, N., Bito, H., Kodama, T., Friedel, R. H., *et al.* (2011) Suppression of bone formation by osteoclastic expression of semaphorin 4D. *Nat.*

- Med.* 17; 1473–1480.
33. Nishikawa, K., Nakashima, T., Takeda, S., Isogai, M., Hamada, M., Kimura, A., *et al.* (2010) Maf promotes osteoblast differentiation in mice by mediating the age-related switch in mesenchymal cell differentiation. *J. Clin. Invest.* 120; 3455–3465.
 34. Okazaki, M., Takeshita, S., Kawai, S., Kikuno, R., Tsujimura, A., Kudo, A., *et al.* (1994) Molecular cloning and characterization of OB-cadherin, a new member of cadherin family expressed in osteoblasts. *J. Biol. Chem.* 269; 12092–12098.
 35. Radice, G. L., Rayburn, H., Matsunami, H., Knudsen, K. A., Takeichi, M. and Hynes, R. O. (1997) Developmental defects in mouse embryos lacking N-cadherin. *Dev. Biol.* 181; 64–78.
 36. Shen, B., Vardy, K., Hughes, P., Tasdogan, A., Zhao, Z., Yue, R., *et al.* (2019) Integrin $\alpha 11$ is an Ostelectin receptor and is required for the maintenance of adult skeletal bone mass. *ELife* 8; e42274.
 37. Stains, J. P. and Civitelli, R. (2005) Cell-cell interactions in regulating osteogenesis and osteoblast function. *Birth Defects Res. C. Embryo Today* 75; 72–80.
 38. Taha, M., Aldirawi, M., März, S., Seebach, J., Odenthal-Schnittler, M., Bondareva, O., *et al.* (2019) EPLIN- α and - β Isoforms Modulate Endothelial Cell Dynamics through a Spatiotemporally Differentiated Interaction with Actin. *Cell Rep.* 29; 1010–1026.e6.
 39. Takayanagi, H. (2007) Osteoimmunology: shared mechanisms and crosstalk between the immune and bone systems. *Nat. Rev. Immunol.* 7; 292–304.
 40. Takeichi, M. (1995) Morphogenetic roles of classic cadherins. *Curr. Opin. Cell Biol.* 7; 619–627.
 41. Wahl, J. K., 3rd, Kim, Y. J., Cullen, J. M., Johnson, K. R. and Wheelock, M. J. (2003) N-cadherin-catenin complexes form prior to cleavage of the proregion and transport to the plasma membrane. *J. Biol. Chem.* 278; 17269–17276.

This is an open access article distributed under the Creative Commons Attribution-NonCommercial 4.0 International License (CC-BY-NC), which permits use, distribution and reproduction of the articles in any medium provided that the original work is properly cited and is not used for commercial purposes.
